Prethermalization and persistent order in the absence of a thermal phase transition

Jad C. Halimeh,[1] Valentin Zauner-Stauber,[2] Ian P. McCulloch,[3] Inés de Vega,[1] Ulrich Schollwöck,[1] and Michael Kastner[4,5]

[1]*Physics Department and Arnold Sommerfeld Center for Theoretical Physics, Ludwig-Maximilians-Universität München, D-80333 München, Germany*

[2]*Vienna Center for Quantum Technology, University of Vienna, Boltzmanngasse 5, 1090 Wien, Austria*

[3]*ARC Centre for Engineered Quantum Systems, School of Mathematics and Physics, The University of Queensland, St Lucia, Queensland 4072, Australia*

[4]*National Institute for Theoretical Physics, Stellenbosch 7600, South Africa*

[5]*Institute of Theoretical Physics, Department of Physics, University of Stellenbosch, Stellenbosch 7600, South Africa*

(Received 7 October 2016; revised manuscript received 16 December 2016; published 6 January 2017)

We numerically study the dynamics after a parameter quench in the one-dimensional transverse-field Ising model with long-range interactions ($\propto 1/r^\alpha$ with distance r), for finite chains and also directly in the thermodynamic limit. In nonequilibrium, i.e., before the system settles into a thermal state, we find a long-lived regime that is characterized by a prethermal value of the magnetization, which in general differs from its thermal value. We find that the ferromagnetic phase is stabilized dynamically: as a function of the quench parameter, the prethermal magnetization shows a transition between a symmetry-broken and a symmetric phase, even for those values of α for which no finite-temperature transition occurs in equilibrium. The dynamical critical point is shifted with respect to the equilibrium one, and the shift is found to depend on α as well as on the quench parameters.

DOI: 10.1103/PhysRevB.95.024302

I. INTRODUCTION

In equilibrium, phase transitions and critical phenomena are well established and much studied, and implications like universality and scaling are well understood. Extending these concepts to nonequilibrium is a topic of active research. Fundamentally different notions of so-called dynamical quantum phase transitions have been proposed, but their mutual relations, and also the associated universality classes and scaling laws, are only poorly understood. In this paper we are concerned with a type of dynamical quantum phase transition that is based on the notion of an order parameter, similar to Landau's theory of phase transitions in equilibrium. The key idea is to identify a dynamical quantum phase transition on the basis of a suitable order parameter in a prethermal regime, i.e., a nonequilibrium regime in which the system may be found before relaxing to thermal equilibrium, and which persists sufficiently long such that a value can be assigned to the order parameter [1–14]. A prethermal state retains some memory of the initial state of the system, therefore the prethermal value of the order parameter will in general differ from its thermal equilibrium value, and it may or may not show symmetry breaking and other signatures associated with the occurrence of a phase transition [15].

A simple protocol for probing such a dynamical quantum phase transition is a quantum quench into the vicinity of an equilibrium quantum critical point. Consider a family of Hamiltonians $H(\lambda) = H_1 + \lambda H_2$, parametrized by $\lambda \in \mathbb{R}$. In equilibrium at zero temperature and some critical parameter value λ_c, a quantum phase transition will in many cases occur, i.e., an abrupt change of the ground-state properties of H. The idea of a quantum quench is to prepare the system in the ground state of $H(\lambda_0)$, and then, starting at time $t = 0$, time-evolve that state under $H(\lambda)$ with $\lambda \neq \lambda_0$. Depending on the quench parameters and the system under investigation, signatures similar to those of the equilibrium phase transition may or may not persist and be visible after the quench, critical properties may be modified, enhanced, or attenuated. Questions of this sort have previously been addressed mostly in mean-field models [5,6] and field theories [7,9,10].

Dynamical quantum phase transitions are expected to be related in some way to their equilibrium counterparts, as they show a similar kind of symmetry breaking and are signalled by the same order parameter. Whether such a relation exists in all cases, and what its precise nature is, is a question that we want to address in this paper. A relation to equilibrium quantum phase transitions at $T = 0$ is supported by the fact that in previous work dynamical quantum phase transitions have been observed by quenching into the vicinity of a quantum critical point. Additionally, a relation to a finite-T phase transition may be conjectured by noticing that a quench populates excited states above the ground state of the postquench Hamiltonian, which generically, at least after sufficiently long times, are expected to approach a thermal distribution with $T > 0$.

II. LONG-RANGE TRANSVERSE-FIELD ISING MODEL

To probe the relation between equilibrium and dynamical quantum phase transitions, we study a model that has a quantum phase transition at zero temperature, and additionally, depending on a parameter, may or may not have a finite-T transition as well. A model that has these desired properties is the transverse-field Ising model (TFIM) with ferromagnetic power-law interactions,

$$H(h) = -\sum_{i>j=1}^{L} \frac{\sigma_i^z \sigma_j^z}{|i-j|^\alpha} - h \sum_{i=1}^{L} \sigma_i^x. \tag{1}$$

We consider one-dimensional lattices consisting of L lattice sites, and σ_i^a with $a \in \{x, y, z\}$ denote the components of Pauli spin-1/2 operators on lattice site i. The exponent α in (1) tunes the range of the spin-spin interaction, from all-to-all coupling at $\alpha = 0$ to nearest-neighbor coupling in the limit $\alpha \to \infty$. We restrict the discussion to exponents $\alpha > 1$, so that an N-dependent scaling factor to make the Hamiltonian (1) extensive is not needed. For all values of α, this model has

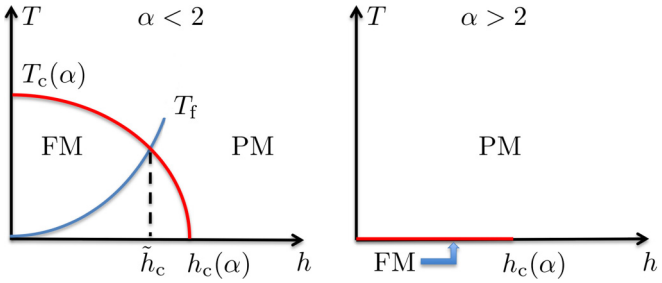

FIG. 1. Schematic phase diagram of the long-range TFIM (1). The model exhibits an equilibrium quantum phase transition at a critical point $h_c(\alpha)$ for all values of α. A finite-T phase transition occurs only for $\alpha < 2$ (left), but not for $\alpha > 2$ (right). Quenching from $h_i = 0$ to $h_f = h$ and letting the system thermalize, equilibrium states on a line $T_f(h)$ (blue line in the left plot) are reached at long times. The phase-transition line is crossed at a field $\tilde{h}_c < h_c(\alpha)$, which results in a shift of the critical field with respect to the quantum critical point.

a quantum phase transition at some critical magnetic field $h_c(\alpha)$, whereas a finite-T phase transition occurs only for $\alpha \leqslant 2$ [16,17] (see Fig. 1 for an illustration).

We use the magnetic field h as a quench parameter, starting in the ground state $|\psi_i\rangle$ of an initial Hamiltonian $H(h_i)$ at time $t = 0$, and then time-evolving that state under the evolution generated by a Hamiltonian $H(h_f)$ with a field h_f different from h_i. We will mainly consider quenches starting from $h_i = 0$, i.e., initial states from the degenerate ground space, where we pick the symmetry-broken, fully polarized state in the $+z$ direction. Our aim is to detect the occurrence of a dynamical quantum phase transition by monitoring the magnetization

$$m(t) = \frac{1}{L}\sum_{j=1}^{L}\langle\psi_i(t)|\sigma_j^z|\psi_i(t)\rangle, \tag{2}$$

where $|\psi_i(t)\rangle = \exp[-iH(h_f)t]|\psi_i\rangle$ is the time-evolved state after the quench.

Except for the extreme cases $\alpha = 0$ and $\alpha = \infty$, the model (1) is nonintegrable, and is expected to thermalize in the long-time limit. Hence, in that limit, the magnetization (2) will show order-parameter-like behavior for $\alpha < 2$, or be vanishing throughout for $\alpha > 2$, as predicted by the phase diagrams in Fig. 1. While thermalization will happen eventually, the corresponding time scale can be extremely long, so long in fact that it may become irrelevant for experimental observations.

III. DYNAMICAL QUANTUM PHASE TRANSITIONS

A dynamical quantum phase transition may be detected by studying the order parameter m as a function of the final quench parameter h_f in a nonequilibrium regime corresponding to intermediate time scales. To generate some intuition on what kind of behavior to expect, it is instructive to consider two limiting cases: (i) For small quenches from $h_i = 0$ to $h_f \gtrsim 0$, excitations above the ground state of $H(h_f)$ are only sparsely populated, the dynamics towards a finite-T thermal state of Hamiltonian will take place very slowly, and a memory of the nonvanishing magnetization of the ground state of $H(0)$ will be retained for a long time. (ii) For a large quench well beyond the critical point, $h_f \gg h_c(\alpha)$, excitations are massively populated, no slow variables are expected to exist, and a rapid approach to $m = 0$ is expected. In between these two extreme cases (i) and (ii), one may expect a transition between a regime with nonvanishing magnetization at small h_f and a regime with vanishing m at large h_f. Such a dynamical quantum phase transition has previously been observed in the TFIM with all-to-all interactions ($\alpha = 0$) [12,18,19], but this case is special in more than one way and its behavior is not expected to be generic.

IV. NUMERICAL METHODS

In this paper we use two complementary numerical methods to study dynamical quantum phase transitions after a quench in the general (nonintegrable) TFIM with long-range interactions (1). The first is the time-dependent density matrix renormalization-group (t-DMRG) [20–27] method with Krylov [28] time evolution, which we apply to finite chains of up to 128 sites. The second is a method based on a time-dependent variational principle for matrix product states [22,29–31], tailored for simulating the dynamics of long-range lattice systems in the thermodynamic limit. Details on this numerical method, which we abbreviate by iMPS, are provided in the companion paper [32]. The combination of the two methods allows us to observe finite-size effects as would be visible in experimental realization on the one side, but also clean infinite-system idealizations as they are used in theoretical approaches. Both numerical methods are certified in the sense that they use well controlled approximations, tunable by an upper bound of the entanglement of the simulated states, which we set to achieve good simulation accuracies. During the simulation we monitor the order parameter m as a function of time (2), as illustrated in Fig. 2 for different quench parameters.

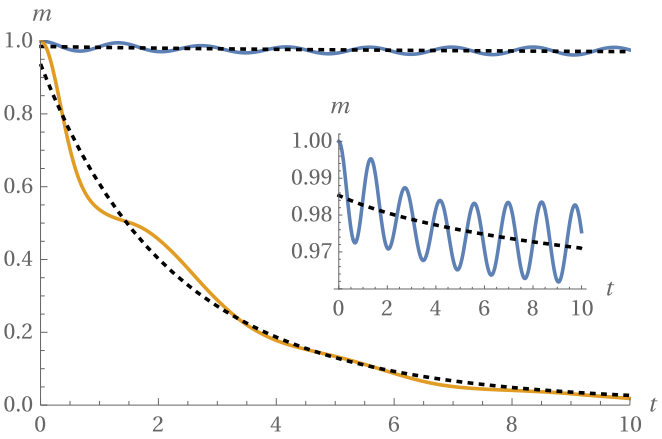

FIG. 2. Time evolution of the order parameter m as obtained from iMPS simulations for long-range exponent $\alpha = 3$. (Data from finite-size t-DMRG simulations look very similar.) For a strong quench from $h_i = 0$ to $h_f = 0.99$, the magnetization quickly decays towards zero (yellow line) and is well approximated by a power law (lower black line). For a small quench from $h_i = 0$ to $h_f = 0.28$, the magnetization shows an initial decay away from its initial value of 1 on a fast time scale (inset), and then saturates to a nonzero value for rather long times (blue line). Eventually, for the chosen parameter values and on a time scale not accessible in simulations, the system will thermalize to a state with zero magnetization.

The time scales that can be reached in the simulation depend on the lattice size L, but also on other system and quench parameters. The simulation methods used are considered the current state of the art for one-dimensional spin systems.

V. THERMAL BEHAVIOR AFTER A QUENCH

Before discussing dynamical quantum phase transitions at intermediate times, it is instructive to review the well-known equilibrium physics of the long-range TFIM [16,17] in the context of quantum quenches and long-time limits. Starting in the ground state corresponding to $h_i = 0$ and quenching to $h_f \neq 0$, the system will not be in the ground state of $H(h_f)$. A nonintegrable model like the one we are studying is then believed to thermalize after a sufficiently long time towards a finite-temperature Gibbs state. The temperature of that state depends on h_f, and this dependence can be described by some function $T_f(h_f)$. This implies that, by performing a quench and waiting sufficiently long for the system to thermalize, one explores the (T,h) equilibrium phase diagram along the line $(T_f(h_f),h_f)$ parametrized by h_f (blue line in Fig. 1). A phase transition will be observed for all $\alpha \leqslant 2$ as predicted by equilibrium thermodynamics, and it will occur at a critical field $\tilde{h}_c$ [corresponding to the value at which $T_f(h)$ crosses the thermal equilibrium transition line] that is smaller than h_c of the quantum phase transition.

VI. DYNAMICAL QUANTUM PHASE TRANSITION OF THE LONG-RANGE TFIM

Quenching and waiting for thermalization to occur is therefore not a way of observing nonequilibrium physics. To probe dynamical features we have to look at shorter time scales. The inset of Fig. 2 indicates that it is indeed reasonable and beneficial to use equilibrium concepts for the description of nonequilibrium observations on intermediate time scales. The magnetization in that plot starts at 1, and quickly decays away from this value to reach a plateau of $\tilde{m} = 0.97$ around which it oscillates for the times reached in simulations. This prethermal value differs from thermal equilibrium, which is known to be $m = 0$ for the parameters used in Fig. 2. The existence of two separate time scales is a key ingredient for making dynamical quantum phase transitions a meaningful concept: a fast time scale, on which the system evolves away from its trivial initial state, is needed, and a much longer time scale on which thermal equilibrium is reached, such that a long-lived almost-constant nonequilibrium value $\tilde{m}$ can be assigned at intermediate times. Our aim is to extract from the simulation data such prethermal magnetization values $\tilde{m}$, which are indicative of the nonequilibrium physics on intermediate time scales relevant in various experimental settings. For some parameter values, the quasistationary value $\tilde{m}$ is clearly visible and easy to extract, while in other cases the limited simulation times require a fit and subsequent extrapolation to later times. These fitting and extrapolation procedures, which are described in more detail in the Appendix, are part of the "definition" we use to extract the prethermal magnetization $\tilde{m}$. While the bare simulation data are essentially free of errors, the fitting procedure introduces some uncertainty, and extrapolation of the fit function to later times can lead to a significant enhancement of these errors in $\tilde{m}$.

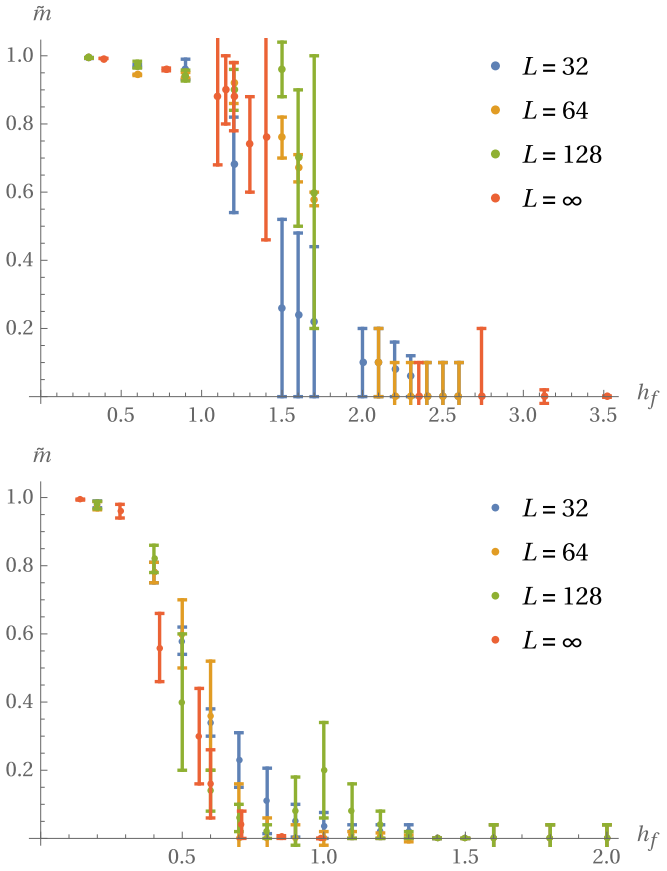

FIG. 3. Prethermal magnetization $\tilde{m}$ plotted as a function of the final quench parameter h_f. Both plots are for quenches starting from $h_i = 0$, and for various system sizes as indicated in the legends. The existence of a magnetized phase for small h_f and an unmagnetized phase for large h_f is clearly visible for $\alpha = 1.6$ (top) and $\alpha = 3$ (bottom).

Plotting the thus obtained prethermal magnetization $\tilde{m}$ as a function of the quench parameter h_f, we find a behavior that is reminiscent of an order parameter; see Fig. 3. Due to the error bars of $\tilde{m}$ it is difficult to determine the precise transition point of this dynamical quantum phase transition on the basis of our numerical data, but we can confirm the existence of a magnetized phase for small quenches, and an unmagnetized phase for large quenches. Remarkably, the magnetized phase is clearly visible also for $\alpha = 3$, and hence the dynamical phase diagram in this case differs drastically from its equilibrium counterpart, which does not have a ferromagnetic phase for $\alpha > 2$. The comparison with iMPS data for infinite lattices confirms that this finding is not a finite-size artefact and indeed persists in the thermodynamic limit. Unfortunately, the (rather conservatively estimated) error bars in Fig. 3 do not allow us to clearly establish whether or not the transition from the magnetized to the unmagnetized phase is indeed a sharp one, or to even extract critical exponents of such a dynamical quantum phase transition. As is evident from Fig. 3, the critical field $\tilde{h}_c$ at which the transition occurs becomes smaller for larger exponents α. This suggests that for such shorter-ranged interactions the prethermalized state can be dynamically stabilized only for smaller quenches, and in that

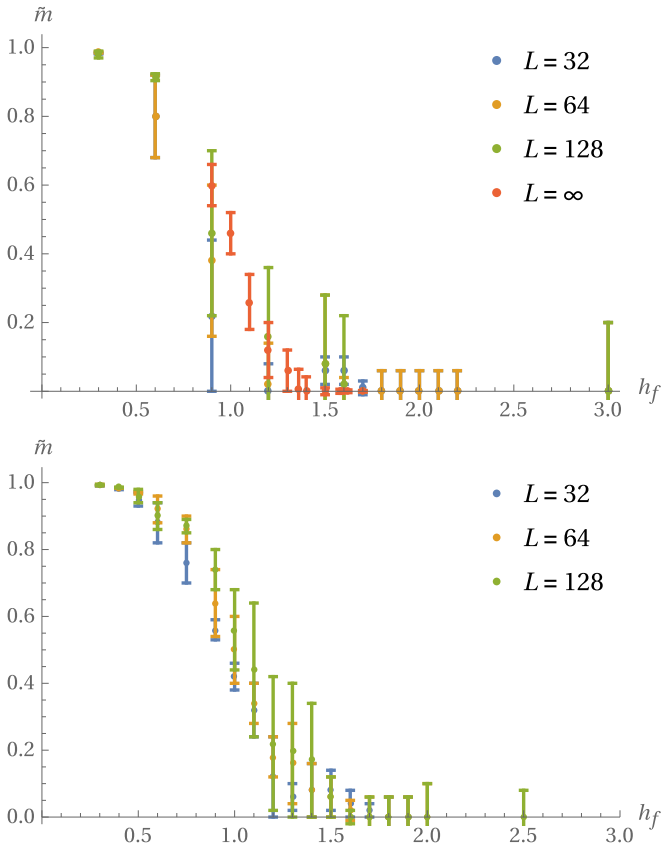

FIG. 4. Prethermal magnetization $\tilde{m}$ plotted as a function of the final quench parameter h_f for $\alpha = 2.3$. Top: quenching from $h_i = 0$; bottom: quenching from $h_i = 0.2$. Both plots show qualitatively similar behavior. A slight dependence of the dynamical critical point on h_i, as expected for the thermal behavior in the long-time limit after the quench, might also be present in the prethermalized regime on intermediate time scales, but cannot be established beyond doubt.

sense the ferromagnetically ordered state is less robust. We expect that $\tilde{h}_c$ approaches h_i in the limit $\alpha \to \infty$, in agreement with the observation that exponential decay to the (generalized Gibbs) equilibrium value sets in immediately in the TFIM with nearest-neighbor interactions.

VII. OTHER TYPES OF QUENCHES

As is usually the case in critical phenomena, the dynamical critical point is expected to be nonuniversal, but to depend on details of the Hamiltonian and, in our case, also on the quench protocol, in particular the initial quench parameter h_i. From the above discussion of the thermal equilibrium behavior after a quench, it appears plausible that also the dynamical critical point $\tilde{h}_c$ should be shifted towards slightly larger values with increasing h_i. To probe this effect, we consider quenches with different prequench Hamiltonians $H(h_i)$, using initial fields $h_i = 0$ and 0.2. In Fig. 4 we show and compare the corresponding dynamical phase diagrams. In both cases the transition from a dynamically ordered to a disordered phase is clearly established, but a shift of the dynamical transition point, if present, is concealed by numerical noise.

It would be interesting to complement the results presented in this paper by studying quenches in the opposite direction, i.e., starting from the fully x-polarized ground state of the Hamiltonian (1) in the limit $h_i \to \infty$ and quenching towards and across the quantum critical point from above. This setting is somewhat more difficult to investigate numerically, as in this case, in addition to the Hamiltonian, the initial state is also $\mathbb{Z}_2$ symmetric. As a consequence, the magnetization is zero for all times and cannot be used to detect a dynamical quantum phase transition. Alternatively, one could use second cumulants of the order parameter as done in Ref. [12], but such a signal is difficult to detect on the basis of limited-time data. Another possibility is to detect critical behavior on the basis of a diverging correlation length, as proposed in Ref. [33], but such an approach is tricky in long-range models, where, even away from criticality, ground-state correlations are in general not exponentially clustered and hence the correlation length is diverging (or ill defined).

VIII. CONCLUSIONS

In summary, we have studied the occurrence of a dynamical quantum phase transition after a quench of the magnetic field in a transverse-field Ising model with long-range interactions. We have provided evidence that a symmetry-broken, ferromagnetic phase can be stabilized dynamically, in the sense that it persists for intermediate times in a prethermalized regime, even in the absence of a ferromagnetically ordered equilibrium phase at finite temperature. Our iMPS variational principle allows us to clearly confirm that such a symmetry-broken phase also persists in the thermodynamic limit. Whether the transition to a symmetric phase with magnetization $\tilde{m} = 0$ is a sharp one, or a smooth crossover, cannot be establish with absolute certainty on the basis of numerical data. So while our results are not fully conclusive on this aspect, the numerical data do not hint at a nonvanishing $\tilde{m}$ for sufficiently large h_f.

We studied the dependence of the dynamical quantum phase transition on model parameters and quench parameters, in particular on the long-range exponent α and the prequench magnetic field h_i. While a specific model was chosen for the numerical study, we expect our findings to be valid more generally for long-range models, also in higher lattice dimension.

The question studied in this paper is a numerically challenging one, and our results are obtained by state-of-the-art implementations of t-DMRG for finite one-dimensional lattices and an iMPS variational principle for infinite lattices. The latter is particularly suited for the problem at hand. An experimental investigation of the phenomena described in this paper should also be feasible: one-dimensional [34,35] or two-dimensional [36] arrays of trapped ions allow for the emulation of long-range interacting Ising spins in a magnetic field and, at least in principle, long-range exponents can be tuned in the range $0 \leqslant \alpha \leqslant 3$ [37]. Preparation of fully polarized initial states as well as parameter quenches are feasible by standard experimental techniques. The required time scales, like in the numerical simulations, are an issue, but do not seem entirely out of reach.

Note added in proof. When finishing up this work we became aware of a preprint by Žunkovič *et al.* [38] that

addresses a similar question, but reaches different conclusions. In particular, the finite-size scaling extrapolations of Ref. [38] are inconsistent with our infinite-system data.

ACKNOWLEDGMENTS

The authors would like to thank P. Calabrese, L. Carr, D. Draxler, M. Eckstein, J. Haegeman, D. Jaschke, S. Kehrein, F. Piazza, and F. Verstraete for fruitful discussions. V.Z.-S. acknowledges financial support by the Austrian Science Fund (FWF), Grants No. F4104 SFB ViCoM and No. F4014 SFB FoQuS. I.P.M. acknowledges support from the Australian Research Council (ARC) Centre of Excellence for Engineered Quantum Systems, Grant No. CE110001013, and the ARC Future Fellowships scheme, FT140100625. I.d.V. acknowledges support by the Nanosystems Initiative Munich (NIM) (Project No. 862050-2). M.K. acknowledges support from the National Research Foundation of South Africa via the Incentive Funding and the Competitive Programme for Rated Researchers.

APPENDIX: FITTING PROCEDURE

When fitting numerical data like those of Fig. 2, the situation can be summarized as follows: We have data of high accuracy, limited to an interval of times up to the order of 10. The data show a decaying tendency, with fairly strong oscillations superimposed, like in the inset of Fig. 2. Our aim is to extrapolate the decay to intermediate times that are, say, an order of magnitude longer than the times t_f reached in the simulations. This time scale of extrapolation is reasonable for several reasons: (i) It is substantially longer than the time scale on which the decay to a prethermalization plateau occurs, hence we look at a time scale that is well separated from the initial dephasing dynamics. (ii) It is at least comparable to the time scales that, with some optimism, might be reached in experimental implementations. (iii) The time scale is short enough such that the error bar that propagates to the extrapolated value is manageable. (Extrapolations to times that are orders of magnitude longer than the simulated times simply become unreliable.)

The main difficulty arises from the fact that the functional form of the decay is not known. Depending on the type of model, quench, and quantity monitored, the decay could be exponential, power law, a combination of both, or something else. To account for this lack of knowledge, we decided to fit a variety of functions to the data,

$$m_1(t) = A\exp(-at), \tag{A1a}$$

$$m_2(t) = A\exp(-at) + c, \tag{A1b}$$

$$m_3(t) = At^{-a}, \tag{A1c}$$

$$m_4(t) = At^{-a} + c, \tag{A1d}$$

$$m_5(t) = A(t - t_0)^{-a}, \tag{A1e}$$

with A, a, c, and/or t_0 as real fit parameters. Using Mathematica's `NonlinearModelFit`, optimal values are returned together with standard error estimates for the fit parameters. The error bars for the fit parameters give us a first indication on which fit functions are suitable for a given data set: If, for a given fit function, one or several of the fit parameters

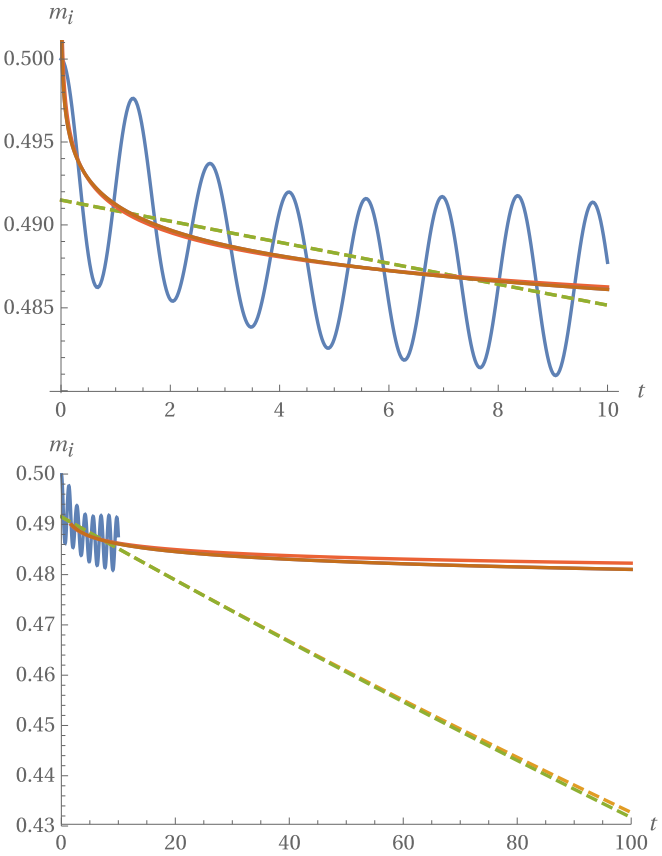

FIG. 5. Illustration of the fitting and extrapolation procedure for $\alpha = 3$, $h_\mathrm{i} = 0$, $h_\mathrm{f} = 0.28$. The oscillating blue line shows the iMPS data. Dashed lines (yellow and green, almost on top of each other and hardly distinguishable on the scale of the plots) show the exponential fit functions m_1 and m_2, solid lines (orange, brown, and purple, again hardly distinguishable) show power law fits m_3, m_4, and m_5. For the three-parameter fits m_2, m_4, and m_5, the optimal values of the fit parameters come with large error bars, and those functions are therefore discarded. Among the two-parameter fits, m_3 (solid orange line) has a significantly smaller mean squared deviation from the simulation data than m_1 (dashed yellow), and is therefore used for determining the prethermal magnetization $\tilde{m} = m_3(10t_\mathrm{f})$.

are afflicted with large relative error bars, the fit function has more parameters than is justified by the data and therefore should be discarded. For the remaining fit functions the accuracy with which they fit the data is assessed on the basis of the mean-squared deviation, and the functions with larger deviations are discarded; see Fig. 5 (top) for an example.

After these two selection steps, depending on the specific data set used, one or several suitable fit functions remain, and those are extrapolated to a time $10t_\mathrm{f}$ (Fig. 5, bottom). The arithmetic mean of the extrapolated values is used to define the prethermal magnetization,

$$\tilde{m} = \sum_i m_i(10t_\mathrm{f}), \tag{A2}$$

where the summation is over those of the fit functions (A1a)–(A1e) that survived the above described selection procedure. The corresponding standard deviation is used as an error

estimate for $\tilde{m}$. It is the lack of knowledge of the functional form of the decay of $m(t)$, and the resulting variety of possible fits, that accounts for the fairly large error bars in Figs. 3 and 4. While the above described fitting and extrapolation procedure clearly contains some arbitrariness, the rather conservative error estimation makes sure that the phase diagrams are not biased by (possibly unjustified) assumptions about the functional form of the decay of $m(t)$ or the extrapolation time.

[1] M. Moeckel and S. Kehrein, Interaction Quench in the Hubbard Model, Phys. Rev. Lett. **100**, 175702 (2008).

[2] M. Eckstein and M. Kollar, Nonthermal Steady States After an Interaction Quench in the Falicov-Kimball Model, Phys. Rev. Lett. **100**, 120404 (2008).

[3] M. Eckstein, M. Kollar, and P. Werner, Thermalization After an Interaction Quench in the Hubbard Model, Phys. Rev. Lett. **103**, 056403 (2009).

[4] M. Moeckel and S. Kehrein, Crossover from adiabatic to sudden interaction quenches in the Hubbard model: Prethermalization and non-equilibrium dynamics, New J. Phys. **12**, 055016 (2010).

[5] B. Sciolla and G. Biroli, Quantum Quenches and Off-Equilibrium Dynamical Transition in the Infinite-Dimensional Bose-Hubbard Model, Phys. Rev. Lett. **105**, 220401 (2010).

[6] B. Sciolla and G. Biroli, Dynamical transitions and quantum quenches in mean-field models, J. Stat. Mech. (2011) P11003.

[7] A. Gambassi and P. Calabrese, Quantum quenches as classical critical films, Europhys. Lett. **95**, 66007 (2011).

[8] N. Tsuji, M. Eckstein, and P. Werner, Nonthermal Antiferromagnetic Order and Nonequilibrium Criticality in the Hubbard Model, Phys. Rev. Lett. **110**, 136404 (2013).

[9] B. Sciolla and G. Biroli, Quantum quenches, dynamical transitions, and off-equilibrium quantum criticality, Phys. Rev. B **88**, 201110 (2013).

[10] A. Chandran, A. Nanduri, S. S. Gubser, and S. L. Sondhi, Equilibration and coarsening in the quantum $O(N)$ model at infinite N, Phys. Rev. B **88**, 024306 (2013).

[11] A. Maraga, A. Chiocchetta, A. Mitra, and A. Gambassi, Aging and coarsening in isolated quantum systems after a quench: Exact results for the quantum O(N) model with $N \to \infty$, Phys. Rev. E **92**, 042151 (2015).

[12] P. Smacchia, M. Knap, E. Demler, and A. Silva, Exploring dynamical phase transitions and prethermalization with quantum noise of excitations, Phys. Rev. B **91**, 205136 (2015).

[13] T. Langen, T. Gasenzer, and J. Schmiedmayer, Prethermalization and universal dynamics in near-integrable quantum systems, J. Stat. Mech. (2016) 064009.

[14] M. Marcuzzi, J. Marino, A. Gambassi, and A. Silva, Prethermalization from a low-density Holstein-Primakoff expansion, Phys. Rev. B **94**, 214304 (2016).

[15] The dynamical quantum phase transition introduced in [39], based on a formal analogy to Fisher zeros in the complex temperature plain for equilibrium transitions, leads to nonanalyticities in time, which is not what we discuss in the present paper.

[16] F. J. Dyson, Existence of a phase-transition in a one-dimensional Ising ferromagnet, Commun. Math. Phys. **12**, 91 (1969).

[17] A. Dutta and J. K. Bhattacharjee, Phase transitions in the quantum Ising and rotor models with a long-range interaction, Phys. Rev. B **64**, 184106 (2001).

[18] A. Das, K. Sengupta, D. Sen, and B. K. Chakrabarti, Infinite-range Ising ferromagnet in a time-dependent transverse magnetic field: Quench and ac dynamics near the quantum critical point, Phys. Rev. B **74**, 144423 (2006).

[19] B. Žunkovič, A. Silva, and M. Fabrizio, Dynamical phase transitions and Loschmidt echo in the infinite-range XY model, Philos. Trans. R. Soc. A **374**, 20150160 (2016).

[20] S. R. White, Density Matrix Formulation for Quantum Renormalization Groups, Phys. Rev. Lett. **69**, 2863 (1992).

[21] U. Schollwöck, The density-matrix renormalization group, Rev. Mod. Phys. **77**, 259 (2005).

[22] U. Schollwöck, The density-matrix renormalization group in the age of matrix product states, Ann. Phys. (NY) **326**, 96 (2011).

[23] S. R. White and A. E. Feiguin, Real-Time Evolution Using the Density Matrix Renormalization Group, Phys. Rev. Lett. **93**, 076401 (2004).

[24] F. Verstraete, J. J. García-Ripoll, and J. I. Cirac, Matrix Product Density Operators: Simulation of Finite-Temperature and Dissipative Systems, Phys. Rev. Lett. **93**, 207204 (2004).

[25] G. Vidal, Efficient Simulation of One-Dimensional Quantum Many-Body Systems, Phys. Rev. Lett. **93**, 040502 (2004).

[26] A. J. Daley, C. Kollath, U. Schollwöck, and G. Vidal, Time-dependent density-matrix renormalization-group using adaptive effective Hilbert spaces, J. Stat. Mech. (2004) P04005.

[27] D. Gobert, C. Kollath, U. Schollwöck, and G. Schütz, Real-time dynamics in spin-$\frac{1}{2}$ chains with adaptive time-dependent density matrix renormalization group, Phys. Rev. E **71**, 036102 (2005).

[28] A. N. Krylov, On the numerical solution of the equation by which in technical questions frequencies of small oscillations of material systems are determined, Izvestija AN SSSR (News of Academy of Sciences of the USSR), Otdel. mat. i estest. nauk **VII**, 491 (1931), in Russian.

[29] F. Verstraete, V. Murg, and J. I. Cirac, Matrix product states, projected entangled pair states, and variational renormalization group methods for quantum spin systems, Adv. Phys. **57**, 143 (2008).

[30] J. Haegeman, J. I. Cirac, T. J. Osborne, I. Pižorn, H. Verschelde, and F. Verstraete, Time-Dependent Variational Principle for Quantum Lattices, Phys. Rev. Lett. **107**, 070601 (2011).

[31] J. Haegeman, C. Lubich, I. Oseledets, B. Vandereycken, and F. Verstraete, Unifying time evolution and optimization with matrix product states, Phys. Rev. B **94**, 165116 (2016).

[32] J. C. Halimeh and V. Zauner-Stauber, Enriching the dynamical phase diagram of spin chains with long-range interactions, arXiv:1610.02019.

[33] E. Nicklas, M. Karl, M. Höfer, A. Johnson, W. Muessel, H. Strobel, J. Tomkovič, T. Gasenzer, and M. K. Oberthaler, Observation of Scaling in the Dynamics of a Strongly Quenched Quantum Gas, Phys. Rev. Lett. **115**, 245301 (2015).

[34] P. Richerme, Z.-X. Gong, A. Lee, C. Senko, J. Smith, M. Foss-Feig, S. Michalakis, A. V. Gorshkov, and C. Monroe, Non-local propagation of correlations in quantum systems with long-range interactions, Nature (London) **511**, 198 (2014).

[35] P. Jurcevic, B. P. Lanyon, P. Hauke, C. Hempel, P. Zoller, R. Blatt, and C. F. Roos, Quasiparticle engineering and entanglement propagation in a quantum many-body system, Nature (London) **511**, 202 (2014).

[36] J. W. Britton, B. C. Sawyer, A. C. Keith, C.-C. J. Wang, J. K. Freericks, H. Uys, M. J. Biercuk, and J. J. Bollinger, Engineered two-dimensional Ising interactions in a trapped-ion quantum simulator with hundreds of spins, Nature (London) **484**, 489 (2012).

[37] D. Porras and J. I. Cirac, Effective Quantum Spin Systems with Trapped Ions, Phys. Rev. Lett. **92**, 207901 (2004).

[38] B. Žunkovič, M. Heyl, M. Knap, and A. Silva, Dynamical quantum phase transitions in spin chains with long-range interactions: Merging different concepts of non-equilibrium criticality, arXiv:1609.08482.

[39] M. Heyl, A. Polkovnikov, and S. Kehrein, Dynamical Quantum Phase Transitions in the Transverse-Field Ising Model, Phys. Rev. Lett. **110**, 135704 (2013).